Triple-Loop Control Configuration for Grid-Connected Inverters

Moria Sassonker Elkayam
Department of Electrical Power Engineering and Mechatronics
Tallinn University of Technology
Tallinn, Estonia
moria.sassonker@taltech.ee

Dmitri Vinnikov
Department of Electrical Power Engineering and Mechatronics
Tallinn University of Technology
Tallinn, Estonia
dmitri.vinnikov@taltech.ee

***Abstract*— Advancements in electrical engineering in the field of power electronics, control and renewable energy are imperative for the human race. The environment and the world economy are dependent upon the future of renewable energy. The resulting reductions in CO_2 emissions improve air quality and ultimately human health. Distributed power generation based on renewable energy, such as solar energy, has developed rapidly due to the increasing concern about the environmental pollution and fossil energy shortage. As the interface between power generation system and grid, the grid-connected converter is essential to convert the generated DC power into high quality AC power suitable for injecting into the grid. This paper concerns with control design of resonant controllers in triple-loop control configuration for single phase and three phase grid-connected inverters based on time-domain analysis for precise tracking in order to achieve fast transient response and reduce grid-current harmonics.**

***Index Terms*—Grid-connected converters, current control, resonant controller, triple-loop.**

I. Introduction

It is well-known that in grid-connected *LCL*-filtered inverters (Fig. 1), current behavior directly sets the exchange of power between the two [1]-[3]. The most commonly used current control configurations are single and double loop control schemes. Recently, several methods have been proposed to enhance system efficiency by modelling triple-loop control architecture for grid-connected inverters [4]-[10]. In triple-loop control scheme the outer loop regulates the grid side inductor current, the middle loop regulates capacitor voltage, and the inner loop regulates either inverter side inductor current or capacitor current, as shown in Fig. 2. Different regulators have been suggested in literature for triple-loop structure, where design of resonant controllers for this structure was barely investigated, especially closed-loop time-domain transient performance analysis.

Since in triple loop-configuration system variables are measured to fed-back to each control loops, when those variables act as disturbances, they can be easily eliminated in the other control loops. In case most of the disturbance measured and appropriately cancelled in corresponding plants, the current\voltage regulation problem reduced to tracking challenge only. Therefore, it would be beneficial to impose transient response based on desired magnitude behavior [11]-[12].

This paper proposes a design of three loops control structure for single phase and three phase inverters in order to achieve fast transient response and reduce grid-current harmonics. As mentioned above, since the disturbances of each loop are already measured, the control strategy will be based on time-domain desired transient response of single resonant controllers, by taking into account actuator delay present in any practical system and the bandwidth limitation caused by the middle and inner loops response delay. Simulation results are given in the preliminary results section, utilizing the proposed control structure on grid-connected three-phase inverter.

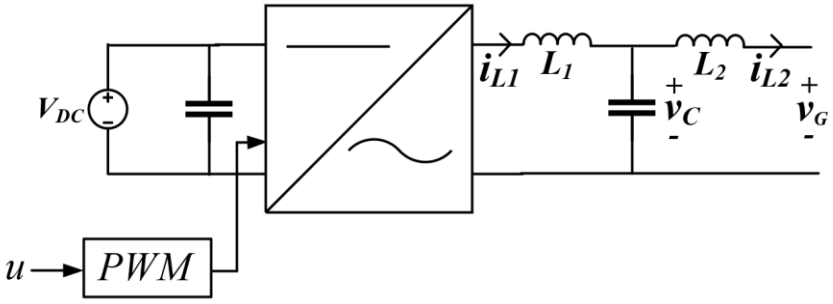

Fig. 1. Typical single-phase inverter representation

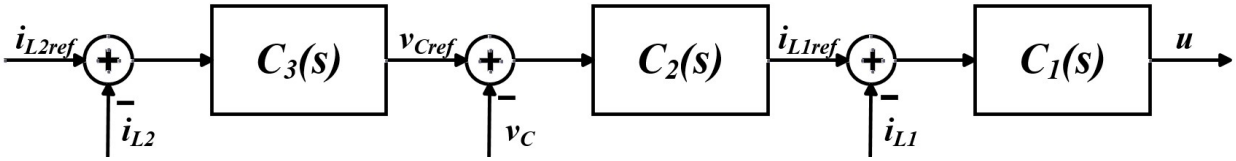

Fig. 2. Block diagram of triple-loop controlled system

II. Proposed Controllers Design

Representation of a grid-connected inverter with *LCL* filter, powered by a DC voltage source v_{DC} is shown in Fig. 2, where u is the controller output (modulating signal), v_G represents the grid voltage and v_C represents the voltage across the filter capacitance. Corresponding plant transfer function for the inner loop may be expressed as,

$$P_1(s) = \frac{i_L(s)}{u(s)} = \frac{1}{R + Ls} e^{-T_d s} \tag{1}$$

where T_d represents the total sampling and transport delay and R is the equivalent series resistance of L. When the inverter is connected to the grid with fundamental frequency ω_0 and/or required to inject sinusoidal current, a single resonant controller is typically utilized. Assume an AC system with reference and output currents with A denoted the amplitude given by

$$\begin{aligned} i_{Lref}(t) &= A \cdot \sin(\omega_0 t) u(t); \\ i_L(t) &= A \cdot \sin(\omega_0 t)\left(1 - e^{-\omega_C t}\right) u(t); \end{aligned} \tag{2}$$

where ω_C is the desired transient performance. Following the design procedure in [12], the resulting single-resonant AC system controller is then given by

$$C(s) = \frac{2\omega_C s + \omega_C^2}{s^2 + \omega_0^2} P(s)^{-1} \tag{3}$$

Combining (1) and (3), the proposed single resonant controller for the inner loop, i.e. inverter side inductor current is then

$$C_1(s) = 2L_1\omega_C + \frac{(L_1\omega_C^2 + 2\omega_C R_1)s + R_1\omega_C^2 - 2L_1\omega_C\omega_0^2}{s^2 + \omega_0^2} \tag{4}$$

For the middle loop, which regulates the capacitor voltage, the plant transfer function is

$$P_2(s) = \frac{V_C(s)}{I_{L1ref}(s)} = \frac{1}{sC} \tag{5}$$

The form of the reference and output capacitor voltage is the same as the current in (2), hence, applying the above design procedure and combining (3) and (5) results in the following middle loop controller

$$C_2(s) = \frac{sC\left(2\omega_{C2}s + \omega_{C2}^2\right)}{s^2 + \omega_0^2} \tag{6}$$

The outer loop is the grid side inductor current loop, which set the capacitor voltage reference value, and the plant is described as

$$P_3(s) = \frac{I_{L2}(s)}{V_C(s)} = \frac{1}{R_2 + L_2 s}, \tag{7}$$

which combining with (3) denotes the following outer loop controller

$$C_3(s) = 2L_2\omega_C + \frac{(L_2\omega_C{}^2 + 2\omega_C R_2)s + R_2\omega_C{}^2 - 2L_2\omega_C\omega_0{}^2}{s^2 + \omega_0{}^2} \tag{8}$$

The resonant transfer function with infinite gain as (3) can cause instability due to limited accuracy in the digital implementation. Therefore, in practical cases, a nonideal transfer function is usually modified with damping factor as follows

$$C(s) = \frac{2\omega_C s + \omega_C{}^2}{s^2 + 2\xi\omega_0 s + \omega_0{}^2} P(s)^{-1} \tag{9}$$

The disturbances of each loop were measured and cancelled by a feed-forward loop. The disturbance of the inner loop is the capacitor voltage, the grid current is the disturbance of the middle loop, and the disturbance of the outer loop is the grid voltage. The feed-forward action is shown in Fig. 4(b) in the results section.

III. Simulation Results

In order to verify the performance of the proposed control structure, simulations were carried out in the PSIM software. The proposed triple loop control structure was applied on three-phase t-type grid connected inverter as shown in Fig. 3. The control algorithm is implemented in *αβ* stationary frame. The measured variables inverter current, grid current, capacitor voltage and grid voltage are transformed using PSIM software from *abc* coordinate to *αβ* coordinate as shown in Fig. 4(a). The resulting proposed control outputs u_α and u_β transform back from the *αβ* coordinate to the *abc* coordinate as shown in Fig. 4(b), section 4. The overall triple loop control algorithm is also shown in Fig. 4(b), where section 3 presents the inner loop proposed control, section 2 the middle loop and section 1 the outer loop proposed control algorithm.

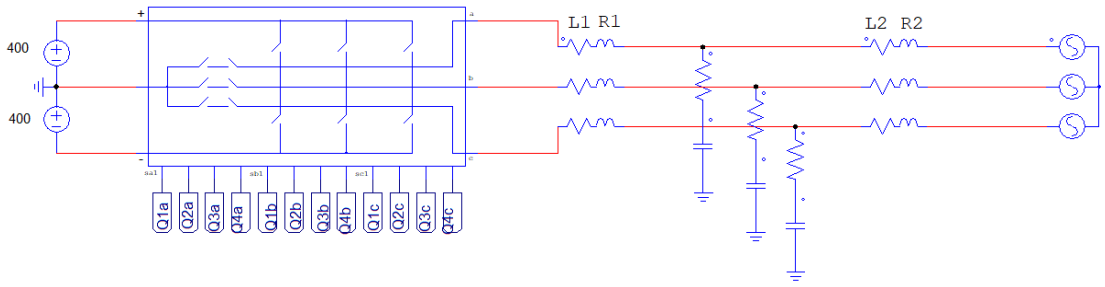

Fig. 3. Simulated T-type grid connected inverter

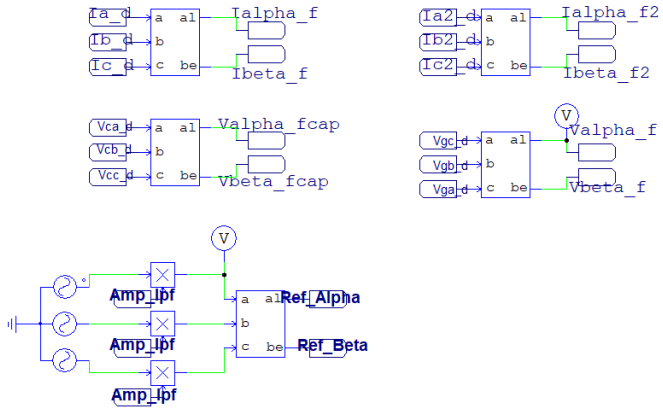

(a)

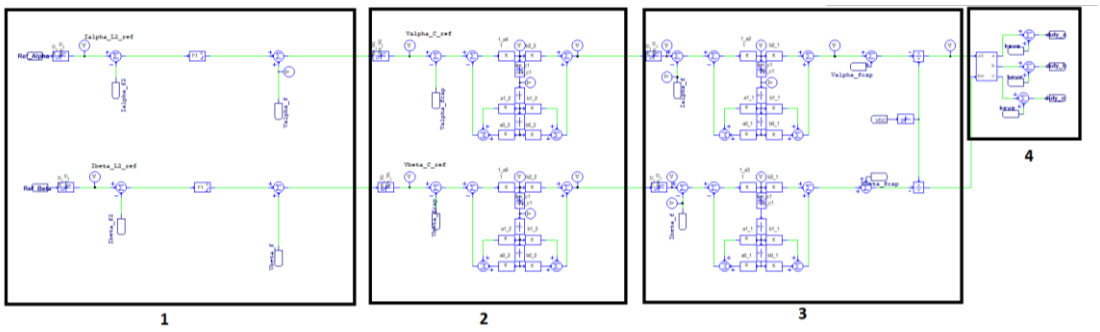

(b)

Fig. 4. Control algorithm implementation in (a) $\alpha\beta$ stationary frame and (b) all triple loop configuration.

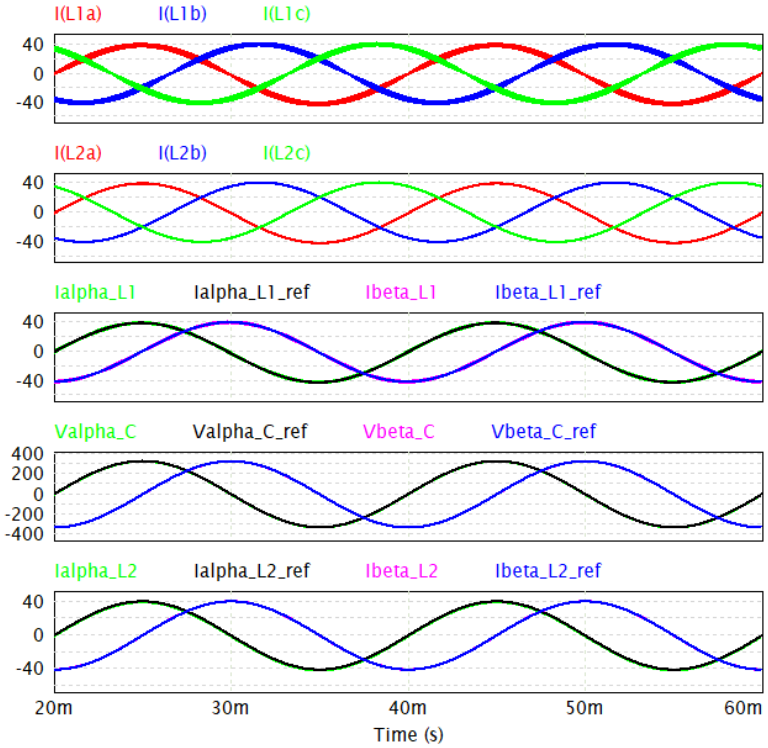

Fig. 5. Simulation results: Three phase inverter (top) and grid side inductors currents, reference and output α and β signals of inverter side inductor current, capacitor voltage and grid current (bottom).

The performance of the proposed control algorithm was examined both in time domain as shown in Fig. 5. The triple loop was applied on both α and β control loops. The results of all three phase inverter and grid side inductors currents are shown from the top, respectively, then the results of reference and output α and β control loops of inverter side inductor current, capacitor voltage and grid current (bottom) are also shown in order to examine tracking performances of proposed controllers. It may be concluded that tracking performance remains satisfactory at all time, demonstrating validity and robustness of the proposed controller.

ACKNOWLEDGMENTS

This research was supported in part by the Estonian Research Council grant PRG1086, and in part by the Estonian Centre of Excellence in Energy Efficiency, ENER (grant TK230) funded by the Estonian Ministry of Education and Research.

REFERENCES

[1] M. Kazmierkowski and L. Malesani, “Current control techniques for three-phase voltage-source PWM converters: A survey,” *IEEE Trans. Ind. Electron*., vol. 45, no. 5, pp. 691 – 703, Oct. 1998.

[2] F. Blaabjerg, R. Teodorescu, M. Liserre and A. Timbus, “Overview of control and grid synchronization for distributed power generation systems,” *IEEE Trans. Ind. Electron*., vol. 53, no. 5, pp. 1398 – 1409, Oct. 2006.

[3] D. Holmes, B. McGrath and S. Parker, “Current regulation strategies for vector-controlled induction motor drivers,” *IEEE Trans. Ind. Electron*., vol. 59, no. 10, pp.3680-3689, Oct. 2012.

[4] S. Buso, T. Caldognetto, and Q. Liu, “Analysis and experimental characterization of large-bandwidth triple-loop controller for grid-tied inverters,” *IEEE Trans. Power Electron.*, vol. 34, no. 2, pp. 1936–1949, Feb. 2019.

[5] Q. Huang and K. Rajashekara, “A unified selective harmonic compensation strategy using DG-interfacing inverter in both grid-connected and islanded microgrid,” in *Proc. IEEE Energy Convers. Congr. Expo.*, Oct. 2017, pp. 1588–1593.

[6] J. He andB.Liang, “Direct microgrid harmonic current compensation and seamless operation mode transfer using coordinated triple-loop current voltage-current controller,” in *Proc. IEEE8th Int.PowerElectron. Motion Control Conf.*, May 2016, pp. 2690–2693.

[7] Z. Yao, L. Xiao, and Y. Yan, “Seamless transfer of single-phase grid interactive inverters between grid-connected and stand-alone modes,” *IEEE Trans. Power Electron.*, vol. 25, no. 6, pp. 1597–1603, Jun. 2010.

[8] J. He and Y.W. Li, “Hybrid voltage and current control approach for DG grid interfacing converters with LCL filters,” *IEEE Trans. Ind. Electron.*, vol. 60, no. 5, pp. 1797–1809, May 2013.

[9] J. He, Y. W. Li, and F. Blaabjerg, “Flexible microgrid power quality enhancement using adaptive hybrid voltage and current controller,” *IEEE Trans. Ind. Electron.*, vol. 61, no. 6, pp. 2784–2794, Jun. 2014.

[10] J. He, B. Liang, Y. W. Li, and C. Wang, “Simultaneous microgrid voltage and current harmonics compensation using coordinated control of dual-interfacing converters,” *IEEE Trans. Power Electron.*, vol. 32, no. 4, pp. 2647–2660, Apr. 2017.

[11] A. Kuperman, "Proportional-resonant current controllers design based on desired transient performance," *IEEE Trans. Power Electron*., vol. 30, no. 10, pp. 5341-5345, Oct. 2015.

[12] M. Elkayam, S. Kolesnik, Y. Basha and A. Kuperman, "Loop shaping by single-resonant controllers for prescribed tracking of sinusoidal references," *IEEE Trans. Power Electron*., vol. 34, no. 11, pp. 11352-11360, Nov. 2019.